JPn Neuroscience

The Journal of Physiology

J Physiol 593.22 (2015) pp 4995–5008

Sleep spindles and human cortical nociception: a surface and intracerebral electrophysiological study

Léa Claude[1], Florian Chouchou[1], Germán Prados[1], Maïté Castro[1], Barbara De Blay[1], Caroline Perchet[1], Luis García-Larrea[1], Stéphanie Mazza[2] and Hélène Bastuji[1,3]

[1] *Central Integration of Pain (NeuroPain) Lab – Neuroscience Research Center, INSERM U1028, CNRS UMR5292, Lyon, France*
[2] *Université Lumière Lyon 2, Laboratoire d'Etude des Mécanismes Cognitifs (EMC), Bron, France*
[3] *Unité d'Hypnologie, Service de Neurologie Fonctionnelle et d'Épileptologie, Hôpital Neurologique, Hospices Civils de Lyon, Bron, France*

Key points

- Sleep spindle are usually considered to play a major role in inhibiting sensory inputs.
- Using nociceptive stimuli in humans, we tested the effect of spindles on behavioural, autonomic and cortical responses in two experiments using surface and intracerebral electroencephalographic recordings.
- We found that sleep spindles do not prevent arousal reactions to nociceptive stimuli and that autonomic reactivity to nociceptive inputs is not modulated by spindle activity.
- Moreover, neither the surface sensory, nor the insular evoked responses were modulated by the spindle, as detected at the surface or within the thalamus.
- The present study comprises the first investigation of the effect of spindles on nociceptive information processing and the results obtained challenge the classical inhibitory effect of spindles.

Abstract Responsiveness to environmental stimuli declines during sleep, and sleep spindles are often considered to play a major role in inhibiting sensory inputs. In the present study, we tested the effect of spindles on behavioural, autonomic and cortical responses to pain, in two experiments assessing surface and intracerebral responses to thermo-nociceptive laser stimuli during the all-night N2 sleep stage. The percentage of arousals remained unchanged as a result of the presence of spindles. Neither cortical nociceptive responses, nor autonomic cardiovascular reactivity were depressed when elicited within a spindle. These results could be replicated in human intracerebral recordings, where sleep spindle activity in the posterior thalamus failed to depress the thalamocortical nociceptive transmission, as measured by sensory responses within the posterior insula. Hence, the assumed inhibitory effect of spindles on sensory inputs may not apply to the nociceptive system, possibly as a result of the specificity of spinothalamic pathways and the crucial role of nociceptive information for homeostasis. Intriguingly, a late scalp response commonly considered to reflect high-order stimulus processing (the 'P3' potential) was significantly enhanced during spindling, suggesting a possible spindle-driven facilitation, rather than attenuation, of cortical nociception.

(Received 14 May 2015; accepted after revision 23 August 2015; first published online 2 September 2015)
Corresponding author H. Bastuji: Unité d'Hypnologie, Service de Neurologie Fonctionnelle et d'Epileptologie, Hôpital Neurologique, Hospices Civils de Lyon, 59 Boulevard Pinel, 69500 Bron, France. Email: helene.bastuji@univ-lyon1.fr

Abbreviations AASM, American Academy of Sleep Medicine; EKG, electrocardiogram; EMG, electromyogram; EOG, electrooculogram; LEP, laser-evoked potentials; MNI, Montreal Neurological Institute; MRI, magnetic resonance imaging; REM, rapid eye movement; SEEG, stereo-electroencephalography.

DOI: 10.1113/JP270941

Introduction

First described by Loomis *et al.* (1935), spindles are transient cerebral activities occurring during non-rapid eye movement (REM) sleep, and appearing on EEG as 'waxing and waning' 12–15 Hz oscillating waves lasting 0.5-2 s (De Gennaro & Ferrara, 2003). According to model of Steriade (2006), spindling is initiated at the cellular level by rhythmic inhibitory oscillations at 12–15 Hz in thalamic reticular gabaergic neurons, which induce recurrent postinhibitory rebound spike bursts in thalamocortical glutamatergic units. These bursts lead cortical neurons to respond at spindle's frequency. Consecutively, cortical feedback to the thalamus synchronizes this oscillation inside the entire thalamocortical network (De Gennaro & Ferrara, 2003; Astori *et al.* 2013).

Despite considerable knowledge about the mechanisms underlying the generation of spindles, their function remains poorly understood and to some extent controversial (Astori *et al.* 2013). Pioneering work by Yamadori (1971), suggested a role as 'sensory gate', useful to preserve sleep by inhibiting sensory input. It has been reported that individuals who generate more spindles also have greater tolerance to noise during a noisy night of sleep (Dang-Vu *et al.* 2010) and that both evoked potentials and haemodynamic (blood oxygen level-dependent) thalamocortical responses become attenuated when pure-tone auditory stimuli are delivered during spindle activity (Elton *et al.* 1997; Cote *et al.* 2000; Dang-Vu *et al.* 2011; Schabus *et al.* 2012). However, such an inhibitory role of sleep spindles has not been supported universally, and Moruzzi *et al.* (1950) were the first to state that 'several types of evoked electro-cortical activities [. . .] undergo pronounced *augmentation* during spindle bursts'. In this respect, two studies in humans failed to show any blockade of sensory or cardiovascular responses to auditory stimuli during spindling (Church *et al.* 1978; Crowley *et al.* 2004), and one of them even suggested that sleep spindles may reflect 'phasic reductions in inhibitory action', resulting in increased transmission of sensory events (Church *et al.* 1978). In the intact cortex of cats, spontaneous spindles were shown to induce increased synaptic responsiveness to single stimuli, suggesting that they might actively induce neural plasticity (Timofeev *et al.* 2002). Thus, the exact role of sleep spindling in the sensory inputs processing remains controversial.

Sleep spindling might have different cortical actions depending on the type, or intensity, of the stimulus received. For example, stimuli within the frequency range of sleep spindles triggered 'augmenting' cortical responses in slabs of cat's cortex when their intensity was relatively high, whereas, at low intensities, cortical responses were decremental (Timofeev *et al.* 2002). Hence, some of the discrepancies reported previously might arise from the use of stimuli with dissimilar behavioural relevance. Nociceptive stimuli are included among those with highest relevance for survival and have a six-fold greater probability of awakening the sleeper than the auditory tones used in most previous studies (Lavigne *et al.* 2004; Bastuji *et al.* 2008); thus, they might provide a straightforward demonstration of the effect of spindles on sleep disruption by external inputs. Also, in contrast to other equally relevant stimuli, nociceptive pulses can be made sufficiently short, in the order of milliseconds, and easily included within or outside the duration of a spindle.

The present study aimed to obtain a comprehensive description of the modulation produced by spindle activity. Accordingly, we assessed behavioural, cortical and autonomic reactions during spindling using phasic nociceptive thermal stimuli. Two all-night experiments were conducted: one with surface EEG recordings in healthy subjects and the other using intracerebral recordings in epileptic patients, in whom detection of spindles within the thalamus was coupled with the recoding of sensory responses in the posterior insula, which is the sensory region responding most systematically to nociceptive stimuli (Garcia-Larrea & Peyron, 2013).

Methods

Subjects

The total sample explored comprised 18 subjects: nine healthy volunteers and nine epileptic patients with implanted intracerebral electrodes. The two experiments were approved by the local Ethics Committee (CCPPRB Léon Bérard-Lyon) and were supported by the French National Agency for Medical Research (INSERM).

Healthy subjects. The nine healthy volunteers (six men, mean ± SD age 30.2 ± 7.4 years) were free of neurological, psychiatric, chronic pain or sleep disorders and were not receiving any psychotropic medication. All subjects provided their informed consent to take part in the experiments, which were conducted in accordance with the Declaration of Helsinki. Subjects were also paid for their participation.

Patients with intracerebral implanted electrodes. The nine patients included in the study (six men, mean ± SD of age 30.9 ± 11.3 years) suffered from partial pharmacoresistant epilepsy. To delineate the extent of the cortical epileptogenic area and to plan a tailored surgical treatment, depth EEG recording electrodes (diameter 0.8 mm; 5–15 recording contacts 2 mm in length, intercontact interval 1.5 mm) were implanted perpendicular to the mid-sagittal plane, in accordance with the stereotactic technique of Talairach & Bancaud (1973). The decision to explore specific areas resulted from the observation

during scalp video-EEG recordings of ictal manifestations suggesting the possibility of seizures either propagating to or originating from these regions (Guenot *et al.* 2001). The thalamus, at or near the pulvinar region, was one of the targets of stereotactic implantation, which, as a result of its reciprocal connections with temporal and parietal cortical areas, may be involved in most of temporal and insular lobe seizures (Rosenberg *et al.* 2009; Bastuji *et al.* 2015). Simultaneous exploration of the thalamus and neocortical areas was possible using a single multicontact electrode, such that thalamic exploration did not increase the risk of the procedure by adding one further electrode track specifically devoted to it. In agreement with French regulations relative to invasive investigations with a direct individual benefit, patients were fully informed with respect to the electrode implantation, stereotactic EEG, evoked potential recordings and cortical stimulation procedures used to localize the epileptogenic cortical areas and all provided their informed consent.

Stimuli

Radiant nociceptive heat pulses of 5 ms in duration were delivered with a Nd:YAP laser (yttrium aluminium perovskite; wavelength 1.34 lm; ElEn, Florence, Italy). The laser beam was transmitted from the generator (outside the bedroom) to the stimulating probe via an optical fibre of 10 m in length (550 μm in diameter with subminiature version A-905 connector; Amphenol Fiber Optic Products, Lisle, IL, USA). Series of laser stimuli were delivered on the dorsum of the right or left hand, alternatively, in healthy subjects, and contralateral to the hemisphere of electrode implantation in patients. The intensity of the laser pulses was kept stable for any given subject during the whole night, slightly above the individual pain threshold obtained at wake. This threshold corresponded to a level of 4–5 on a verbal numerical scale ranging from 0 to 10 (where 0 = no sensation and 10 = unbearable pain; with the intermediate levels being: 1 = barely perceived; 2 = lightly pricking, not painful; 3 = clearly pricking, not painful; 4 = barely painful, like pulling a hair; 5 = painful, prompting to rub the skin; 6 = very painful and distressing; 7 and more = strongly unpleasant pain). Pain thresholds were obtained in all subjects with energy densities of 50–79 mJ mm^{-2}. These pain threshold values were within the normal range of data classically obtained in our laboratory, and are in accordance with the reported experimental data using Nd:YAP lasers (Leandri *et al.* 2006; Perchet *et al.* 2008). To avoid damaging the skin, habituation and peripheral nociceptor fatigue, stimulus blocks consisted of a maximum of 20 laser pulses and the heat spot was slightly shifted over the skin surface after each stimulus (Schwarz *et al.* 2000). The targeting of laser and the slight repositioning were carried out manually, keeping a stable distance to obtain a 4 mm spot, and slightly moving the spot between two stimuli within the hand dorsum, in the territory of the superficial branch of the radial nerve (Cruccu *et al.* 2008). Because preliminary studies showed that delivering stimuli at short (<6 s) and constant intervals increased the probability of awakening (Bastuji *et al.* 2008, 2012), the interstimulus interval was pseudorandomly adjusted online at a minimum of 10 s.

Recording procedures

Surface recordings. All-night electrophysiological recordings were obtained using Ag/AgCl electrodes, mounted on a cap (Quick-Cap 32 electrodes; Compumedics Ltd, Abbotsford, Australia) designed for the extended International 10–20 System. All electrodes were referred to the nose. The electrooculogram (EOG) was recorded with two electrodes placed close to the superolateral right canthus, and the electromyogram (EMG) was recorded using two electrodes over the mentalis muscle in the chin. Electrocardiogram (EKG) and limb movements (limb-EMG) were monitored with an electrode placed on the extensor digitorum communis of the left forearm. All electrodes were connected to the system reference. Ground was placed on the mid-forehead. Skin impedance was maintained <5 kohm. The EEG signal was amplified 30,000 times (SynAmps; Compumedics Ltd) and analogically filtered online (band pass –3 dB/oct, 0.1–70 Hz), then digitized at 500 Hz. Electroencephalogram, EOG, EMG and EKG were recorded continuously between 22.30 h and 07.00 h, and stored for offline analysis.

Intracerebral recordings. Data acquisition was performed in the Functional Neurology and Epileptology Department (Lyon Neurological Hospital). Full night recording sessions with implanted electrodes were performed after 5–10 days of continuous stereo-electroencephalography (SEEG) monitoring in the patients' own rooms. At that time, any 'first-night' effect had faded away, and anti-epileptic drugs had been tapered down so that all patients were under mono- or bitherapy (carbamazepine, valproate, lamotrigine, levetiracetam and pregabalin) with daily dosages at, or slightly under, the minimum of their usual therapeutic range. Online SEEG recordings (Brain-Quick; Micromed, Mâcon, France) were obtained using a 128 channel amplified device at a sampling frequency of 256 Hz and a bandpass filter of 0.03–100 Hz, in both bipolar and referential modes. The reference electrode was chosen for each patient on an implanted contact located in the skull. Blinks and saccades were recorded with two EOG electrodes placed on the supero- and inferolateral right canthus. SEEG, EOG and EKG were recorded continuously during the night and were stored for offline analysis.

Experimental procedure. After estimation of pain thresholds to laser, two separate recording runs of 10–15 stimuli applied to the dorsum of the hand were performed to obtain the waking-laser-evoked-potentials (LEP). Then, the participants (healthy subjects or patients) were allowed to sleep at their own time. Before delivering any further laser stimulation, a minimum of 20 min of continuous sleep was allowed from the first EEG signs of sleep onset. The identification of the different sleep stages was carried out online by an investigator who was an expert in sleep scoring (HB). This allowed stimulation in each sleep stage, and the immediate discontinuation of the sequence if one stimulus awoke the sleeper. In both experiments, stimulations were performed by blocks of a maximum of 20 stimuli throughout the night, in both non-REM and REM sleep. A second investigator entered the bedroom and kept the laser stimulator pointed to the adequate target when the first investigator triggered nociceptive stimuli. The 10 m optical fibre transited under the door separating the recording and sleeping areas and allowed conveniently stimulation of the dorsum of the hand despite any movements of the subjects during the night. Both the sleeping subject and the investigator inside the bedroom wore eye protection.

Data analysis

Sleep analysis. For scalp recordings, sleep stages were visually scored offline according to the American Academy of Sleep Medicine (AASM) (Iber *et al.* 2007). AASM criteria adapted to intracerebral recordings (Magnin *et al.* 2004; Bastuji *et al.* 2012) were used for SEEG data. Hypnograms based on 30 s epochs allowed determination of the vigilance state when stimuli were delivered. As already observed in previous studies, laser stimuli delivered during N3 quite systematically induced a shift to N2 sleep stage (Bastuji *et al.* 2008, 2012) and so only recordings from sleep stage N2 are reported for the present study. Responses to stimuli delivered after less than 1 min of continuous sleep were rejected.

In accordance with the AASM criteria adapted for intracerebral recordings (Bastuji *et al.* 2012), 'cortical arousals' were defined as bursts of waking cortical activity lasting at least 3 s, and 'awakenings' as more than 15 s. These arousal reactions (cortical arousal and awakening) were considered as stimulus-related if occurring within 10 s after stimulus onset. Responses to stimuli delivered during an arousal period were rejected.

Detection of sleep spindles was performed on mid-line FCz-Cz-CPz electrodes in control subjects and on the posterior thalamic contacts in patients with intracerebral electrodes (Fig. 1). On surface recordings, only spindles present in all three electrodes were taken into account (Fig. 2). To identify spindles unambiguously, the EEG signal was bandpass filtered between 12 and 16 Hz (–3 dB down, roll-off –48 dB/oct). Signal was then segmented 5 s before and 5 s after each stimulus. For each of these 10 s epochs, spindles were visually detected on the EEG as a brief distinct bursts of activity in the sigma range (determined using Morlet wavelet analysis) (Fig. 1), lasting at least 0.3 s and with an amplitude value >2 SDs from mean baseline on filtered EEG (for a comparison between automatically and visually spindle detection, see Warby *et al.* 2014).

Anatomical localization of the recording sites. Co-ordinates of relevant targets were determined on the patient's brain magnetic resonance images (MRI) in accordance with procedures described previously (Ostrowsky *et al.* 2002; Frot *et al.* 2014). In five patients implanted before 2010, MRI could not be performed with electrodes in place because of the physical characteristics of the stainless steel contacts. In these cases, the scale 1:1 post implantation skull radiographs performed within the stereotactic frame were superimposed on the pre-implantation scale 1:1 MRI slice corresponding to each electrode track, thus permitting each contact to be plotted onto the appropriate MRI slice of each patient (MRIcro® software; http:/www.mricro.com) (Rorden & Brett, 2000) and its co-ordinates determined. In the other four patients, the implanted electrodes were MRI compatible and both thalamic and cortical contacts could be directly visualized on the post-operative 3-D MRIs. In both cases, anatomical scans were acquired on a 3-Tesla Siemens Avanto Scanner (Siemens AG, Munich, Germany) using a 3-D magnetization-prepared rapid gradient-echo sequence with parameters: TI/TR/TE 1100/2040/2.95 ms, voxel size: $1 \times 1 \times 1$ mm^3, FOV $= 256 \times 256$ mm^2. Each contact, and particularly those exhibiting the largest LEP amplitudes, were then localized in the standard stereotaxic space (Montreal Neurological Institute; MNI). The range of co-ordinates of insular contacts was 31– 40 mm for the *x*-axis, +11 and –24 mm for the *y*-axis and +14 and –5 mm for the *z*-axis.

The localization of contacts within the thalamus was performed superimposing the appropriate MRI slice of each patient on the corresponding plate of Morel's stereotactic atlas of the human thalamus (Morel *et al.* 1997). The range of co-ordinates was 7–16 mm lateral to the mid-line for the *x*-axis, 3 mm rostral to 7 mm caudal to posterior commissural for the *y*-axis and 3–8 mm above anterior commissural/posterior commissural for the *z*-axis (Fig. 1).

Autonomic responses. EKG signals were subjected to peak-to-peak analysis to detect the QRS complex (R waves) using a dedicated Matlab software (MathWorks, Natick, MA, USA). Initial automatized extraction of EKG data was subsequently checked by visual inspection, so that

undetected QRS, ectopic beats or artefacts were corrected, and selected EKG segments were eliminated, if correction was not possible. Periods for EKG RR analysis comprised 40 RR intervals before and 40 RR intervals after each laser stimulus (Chouchou *et al.* 2011).

Evoked potentials. The analysis was performed using BrainVision Analyser (BrainProducts GmbH, Gilching, Germany). Each stimulus delivered during sleep stage N2 was classified as occurring during a sleep spindle [Spindle (S) condition] or apart from a sleep spindle [No Spindle (NS) condition] (Fig. 1). A stimulus was classified as belonging to the S condition when delivered between 300 ms after the beginning and 300 ms before the end of the spindle. A stimulus was classified as belonging to the NS condition when delivered 1000 ms before or after a spindle.

The continuous EEG signal was segmented into epochs beginning 100 ms before and 900 ms after each stimulus. After applying a 0.5–30 Hz bandpass filter, epochs were baseline corrected according to the pre-stimulus period. For each subject, LEPs were averaged according to the stimulus condition (S or NS) (Fig. 2). The number of stimuli delivered in the S condition was smaller than in the NS condition; thus, to obtain averages with similar signal-to-noise ratio in both conditions, in each subject and patient, the number of NS stimuli considered for analysis was reduced to that of S stimuli by selecting the NS stimulus immediately preceding or following each S stimulus and removing of the analyses the remaining NS stimuli. This mode of selection maintained, in both conditions, stimuli delivered in similar periods throughout night.

Scalp responses. Before averaging, epochs presenting movements or artefacts were excluded from the analyses. The different LEP components, N2, P2 and P3, were identified according to their polarities and peak latencies. N2 and P2 corresponded to the vertex negative–positive complex arising within a 200–400 ms window following a laser nociceptive stimulus (Cruccu *et al.* 2008). The first scalp positivity with centro-parietal distribution, following the vertex complex within 350–700 ms was

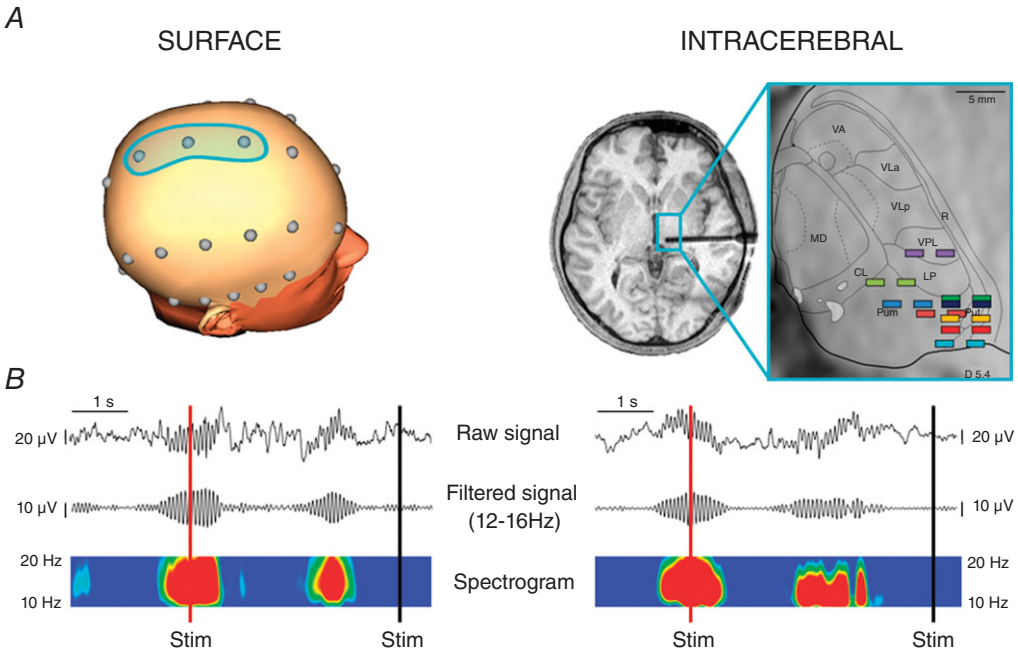

Figure 1. Sleep spindle detection on surface and intracerebral recordings
A, left: 3-D head representation showing the fronto-centro-parietal electrodes where spindle detection was conducted by surface recordings. Right: localization of thalamic contacts used for spindle detection in intracerebral recordings. Contacts were localized on horizontal magnetic resonance images and superimposed on the corresponding dorsoventral horizontal planes of the stereotaxic Morel's atlas (Morel *et al.* 1997) with the posterior commissure level as reference. Each colour of contact pairs depicts implantation site in one given thalamic patient. The thalamic plane illustrated, located 5.4 mm above the anterior commissure-posterior commissure horizontal plane, corresponds to the average level of the nine contact pairs. CL, central lateral nucleus; LP, lateral posterior nucleus; MD, mediodorsal nucleus; PuM, medial pulvinar; PuL, lateral pulvinar; R, reticular thalamic nucleus; VA, ventral anterior nucleus; VPL, ventral posterior lateral nucleus; Vla, ventral lateral anterior nucleus; VLp, ventral lateral posterior nucleus. *B*, examples of raw EEG signals, filtered signals (–48 dB/oct, 12–16 Hz) and wavelet transformed spectrograms on surface (left) and thalamic (right) recordings: nociceptive stimuli are represented as red (spindle) or black (no spindle) vertical lines.

defined as 'P3'. When more than one peak was present within the detection window, we followed the International Federation of Clinical Neurophysiology recommended standards and determined the latency by extrapolation of the ascending and descending limbs of the waveform (Goodin *et al.* 1994). The latencies of N2, P2 and P3 components were measured at the most negative and positive peaks within a latency window encompassing the corresponding waveform. The P3 amplitude was measured peak-to-peak from the preceding negative wave.

Intracerebral responses. LEPs were recorded in the insular cortex, which is the main cortical sensory target of nociceptive (spinothalamic) afferents in primates, including humans (Garcia-Larrea & Peyron, 2013). When several insular contacts were available, the one with the largest response was selected. Seven patients had a contact on the posterior long gyrus and two had a contact on the posterior and middle short gyrus of the insula.

Prior to averaging, epochs presenting epileptic transient activities or artefacts (i.e. voltage deflections exceeding

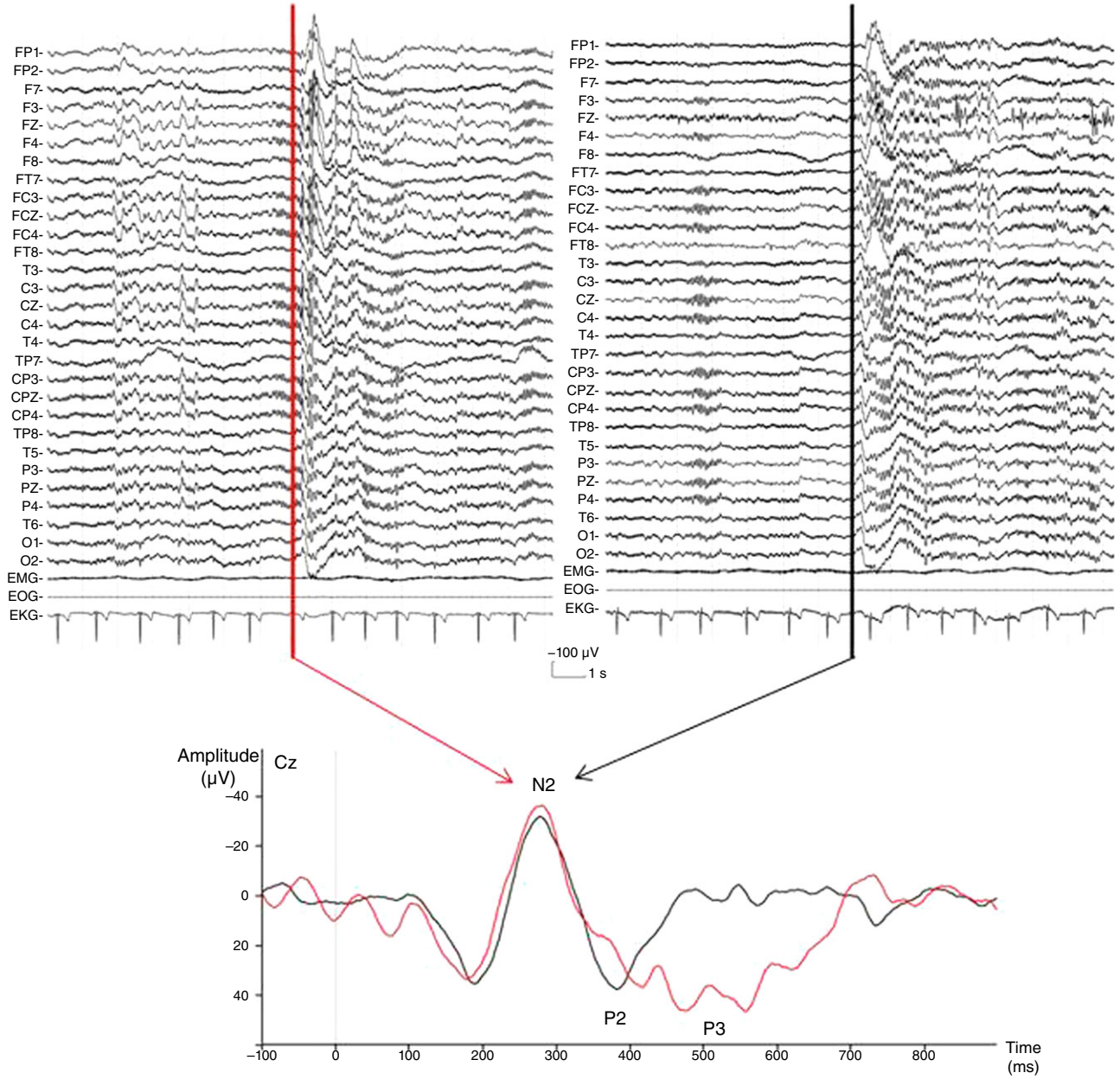

Figure 2. Data from a representative subject illustrating the averaging process
Top: raw traces obtained with two laser stimuli; one delivered during a spindle (left) and another apart from it (right). The upper traces correspond to the EEG and the three bottom traces to chin EMG, EOG and EKG. The vertical lines indicate the laser stimuli (5 ms duration). Bottom: superposition of evoked responses obtained at Cz after averaging from laser stimuli delivered during sleep spindles (red traces) or apart from it (black traces).

100 μV) were rejected from analysis. The insular response to nociceptive stimuli in humans comprised two main components, which were labelled C1 and C2. Because the polarity of the insular responses recorded intracerebrally may vary with the position of the recording lead, the insular responses were not labelled according to polarity but rather as their order of occurrence, as Component 1 (C1) and Component 2 (C2), in accordance with the nomenclature of Bastuji *et al.* (2012). Latencies of each component and peak-to-peak amplitudes were determined on individual averages of each patient. Additionally, to detect any significant amplitude difference at latencies later than the main C1–C2 components, the mean signal amplitude was also compared between the two stimulus conditions in six contiguous 50 ms time windows within the 300–600 ms post-stimulus period.

Statistical analysis. Statistical analysis was performed using Prism, version 6.0 (GraphPad Software Inc., San Diego, CA, USA). For each variable of interest, normality of distribution was tested using the D'Agostino and Pearson normality test. $P < 0.05$ was considered statistically significant. Data are presented as the mean $\pm$ SEM.

Behavioural data. For each subject and patient, the incidence of cortical arousal and awakening was calculated in the Spindle and No Spindle conditions. Data were then submitted to a repeated measures ANOVA with two factors: stimulus condition (Spindle and No Spindle, within factor) and group experiment (Surface and Intracerebral, between factor). A complementary repeated measures analysis of variance (ANOVA) was performed with two within factors: stimulus condition (Spindle and No Spindle) and arousal reaction (Cortical arousal and Awakening).

Autonomic data. To take into account the intersubject variability of the cardiac reactivity latency, as previously reported, for each subject, comparisons were performed on the mean of the three shorter RR intervals between two and seven heart beats post-stimulation (mean RR) compared to the mean of the 5 RR intervals pre-stimulation (Chouchou *et al.* 2011). Mean RR values were submitted to repeated measures ANOVA with two within factors: time (before and after stimulus) and stimulus condition (Spindle and No Spindle). *Post hoc* tests with Sidak's multiple comparisons test were performed when ANOVA yielded significant results.

Electrophysiological data. To achieve data reduction, for each subject, the responses from the 32 electrodes used for scalp recordings were collapsed into three groups of different topography, respectively 'Frontal' (average of values from F7-F3-Fz-F4-F8 electrodes), 'Central' (average of values at T3-C3-Cz-C4-T4 electrodes) and 'Parietal' (average of values at T5-P3-Pz-P4-T6 electrodes). Latencies and amplitudes of each component of scalp LEPs (N2, P2, P3) were then submitted to repeated measures ANOVA with two within factors: stimulus condition (Spindle *vs.* No Spindle) and 'response topography' (Frontal *vs.* Central *vs.* Parietal). *Post hoc* tests with Sidak's multiple comparisons test were performed when ANOVA yielded significant results.

In the intracerebral experiment, because the insular signals showed a high between-subject heterogeneity in amplitude, traces from each patient were normalized using the standard score unit (Z-score), and such standardized traces were used for statistical analyses and presentation of the grand averages. Latencies and peak-to-peak amplitudes of the C1 and C2 insular components between the two stimulus conditions were compared using Student's paired t tests. A comparison of amplitudes in the 'late' time window following the main components (300–600 ms) was performed with repeated measures ANOVA with two within factors: stimulus condition (Spindle and No Spindle) and time window (six contiguous 50 ms time windows spanning the 300–600 ms period).

Results

After artefact rejection, a total of 482 laser stimuli delivered during sleep stage N2 were eligible for analysis: 156 were delivered during a sleep spindle (Spindle condition; S) (surface experiment: 82; intracerebral experiment: 74) and 326 apart from a spindle (No Spindle condition; NS) (surface experiment: 162; intracerebral experiment: 164). Briefly, as shown in Figs 1 and 2, spindles were detected on FCz-Cz-CPz electrodes (surface experiment) or on thalamic contacts (intracerebral experiment) and a similar number of stimuli in S and NS conditions was maintained in each participant. Accordingly, the mean number of stimuli kept for the analysis was 9.1 $\pm$ 1.6 stimuli in each of stimulus conditions per subject in the surface experiment and 8.2 $\pm$ 1.5 in the intracerebral experiment.

Behavioural responses

The percentage of arousal reactions to nociceptive laser stimuli did not differ significantly between the two conditions ($F_{1,8} = 0.86$; $P = 0.37$), nor between the surface and intracerebral experiments ($F_{1,8} = 2.74$; $P = 0.12$), with no interaction ($F_{1,8} = 1.45$; $P = 0.25$). Arousal reactions occurred after 29 $\pm$ 7.3% of the stimuli delivered during an ongoing spontaneous spindle and after 34 $\pm$ 6.65 of those delivered apart from a spindle.

A complementary analysis was performed to determine whether the presence of spindle affected the duration of arousal reactions. This analysis, including subjects of the two studies, showed that cortical arousals (3–15 s) were significantly more frequent than awakenings (> 15 s) after a laser stimulus ($F_{1,17} = 4.74$; $P = 0.0439$; cortical arousal: $22 \pm 4.1\%$ and awakening: $10 \pm 4.0\%$). This phenomenon appeared to be independent of the presence of a spindle simultaneously to the nociceptive stimulation because the interaction between the two factors was not significant ($F_{1,17} = 1.71$; $P = 0.21$).

Autonomic responses

Two-way ANOVA showed that mean cardiac RR interval was significantly modified as a function of time ($F_{1,8} = 23.05$; $P = 0.0014$) but not of the stimulus condition (S/NS) ($F_{1,8} = 0.03$; $P = 0.61$), with no interaction ($F_{1,8} = 0.55$; $P = 0.48$). The mean cardiac RR interval was significantly decreased) (i.e. heart rate increase, following the nociceptive stimuli compared to pre-stimulus period; before: 1139 ± 31 ms; after: 992 ± 34 ms) (Fig. 3).

Laser-evoked responses

Scalp recordings. In the surface experiment, the sensory N2–P2 responses and the late positivity following P2, labelled P3 wave, were considered. No significant difference was detected between the S and NS stimulus conditions for N2 and P2 latencies (N2: $F_{1,8} = 0.07$; $P = 0.8$; P2: $F_{1,8} = 1.69$; $P = 0.23$), nor for N2–P2 amplitude ($F_{1,8} = 1.74$; $P = 0.22$). A significant effect of electrode position (topography) was observed on the N2–P2 amplitude ($F_{2,16} = 11.26$; $P = 0.0009$), which was smaller on frontal electrodes than on central ($t_{16} = 4.07$; $P = 0.0027$) and parietal recordings ($t_{16} = 4.15$; $P = 0.0023$) (Fig. 4 and Table 1). These topographical changes were independent of the existence or not of a concomitant spindle, as shown by the absence of interaction between topography and spindle condition ($F_{2,16} = 0.71$; $P = 0.51$) (Fig. 4 and Table 1).

The latency of the P3 component was not significantly different in the S and NS stimulus conditions ($F_{1,8} = 1.13$; $P = 0.32$). Conversely, the P3 amplitude was significantly different between the two conditions, and higher when the stimulus was delivered during a spindle (S condition:

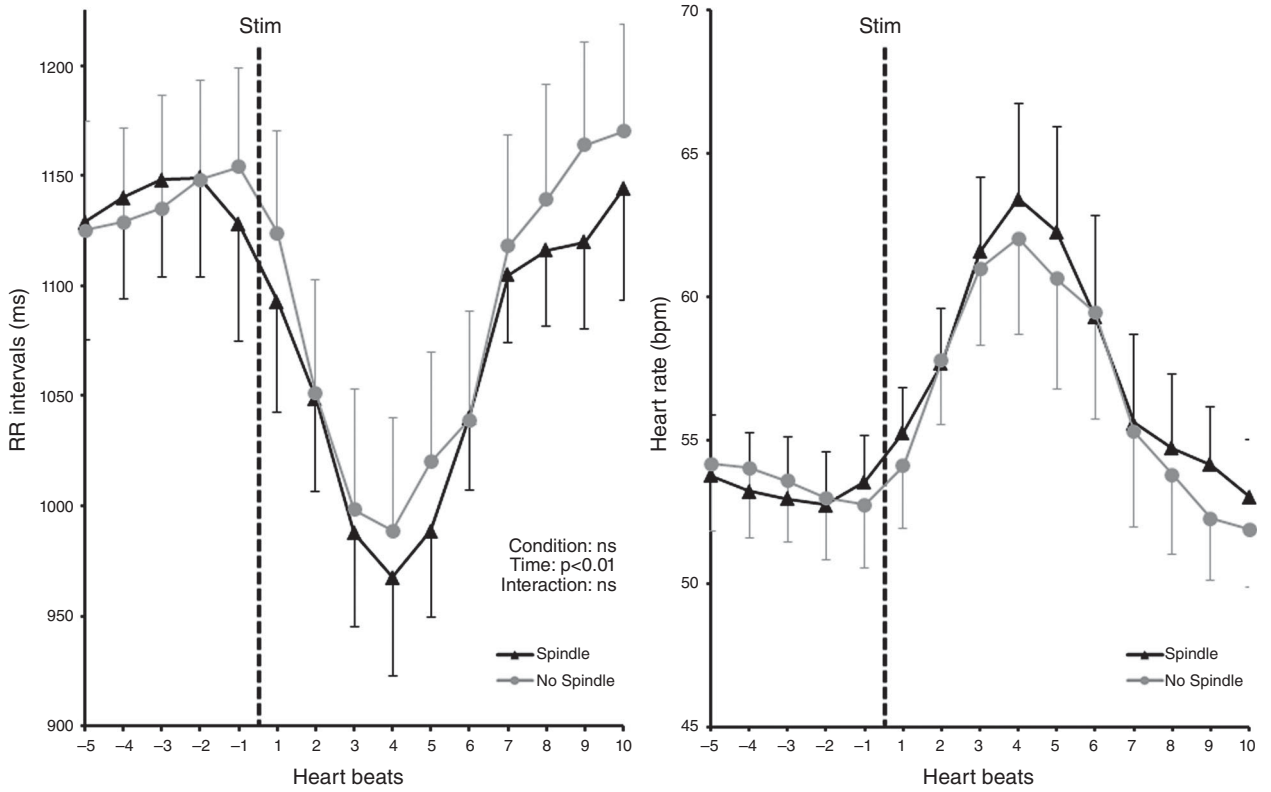

Figure 3. Autonomic responses (mean ± SEM) to laser nociceptive stimuli delivered during (black) and apart from (grey) sleep spindles
Left: cardiac R-R interval evolution preceding and following nociceptive stimuli. Statistical analysis was performed on these data. Right: representation of the same data in heart rate (bpm). Nociceptive stimuli induced a similar R-R interval decrease (i.e. heart rate increase) in both conditions.

19.74 ± 4.38 μV; NS condition: 11.56 ± 1.00 μV; $F_{1,8} = 8.41$; $P = 0.0199$). A significant topography effect was also observed ($F_{2,16} = 5.29$; $P = 0.0172$) with a smaller P3 amplitude on frontal than parietal electrodes ($t_{16} = 3.2$; $P = 0.0166$), as well as a significant interaction between condition and topography ($F_{2,16} = 8.88$; $P = 0.0026$). *Post hoc* tests showed that P3 amplitude was higher in the S condition on central ($t_{16} = 4.32$; $P = 0.0016$) and parietal ($t_{16} = 6.96$; $P < 0.0001$) electrodes (Fig. 4 and Table 1).

Intracerebral recordings. In the intracerebral experiment, the evoked responses analysed within the posterior insula presented two sensory components: C1 and C2. No significant differences between S and NS conditions were detected in the latencies of C1 and C2 (C1: $t_8 = 1.16$; $P = 0.28$ and C2: $t_8 = 1.86$; $P = 0.10$) and C1–C2 amplitude ($t_8 = 0.47$; $P = 0.65$) (Fig. 5 and Table 2). Similarly, no difference between S and NS conditions was observed in the mean amplitudes of late responses (300–600 ms; $F_{1,8} = 0.68$; $P = 0.43$), nor among the six consecutive 50 ms time windows ($F_{5,40} = 0.41$; $P = 0.84$), without any interaction ($F_{5,40} = 0.53$; $P = 0.75$).

Discussion

Sleep spindles, detected during the N2 sleep stage at either the cortical or thalamic level, had no inhibiting effect on arousal, autonomic or cortical responses to nociceptive stimuli. The assumption that spindles have a sleep-protecting role against external inputs (Yamadori, 1971; Steriade, 2006) was not supported by the results of the present study because both the percentage of

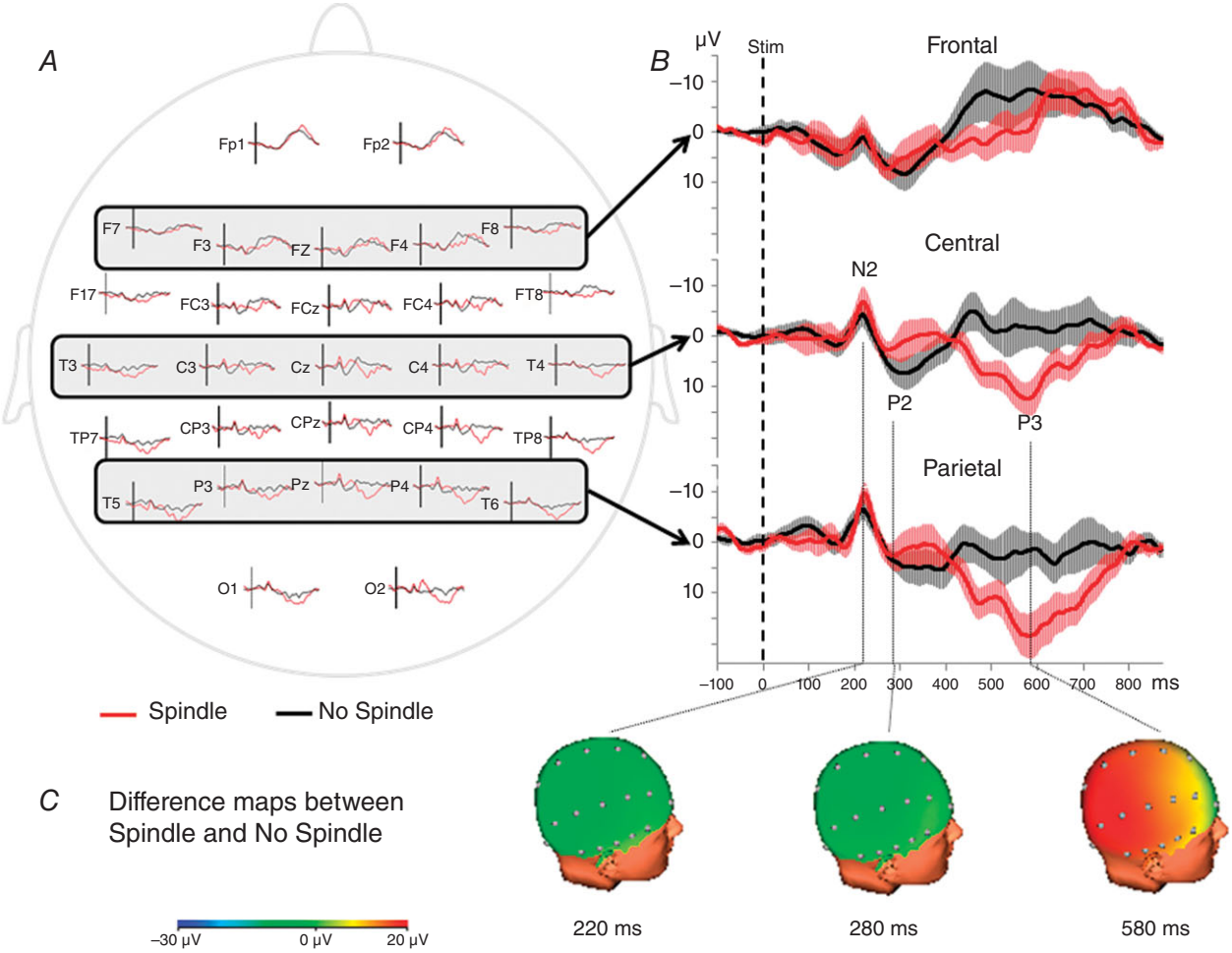

Figure 4. Grand-averages of surface LEPs (n = 9 subjects) according to the stimulus condition (spindle, red traces; no spindles, black traces)
A, surface distribution of LEPs. ***B***, traces obtained in frontal, central and parietal areas, by averaging respectively F7-F3-Fz-F4-F8, T3-C3-Cz-C4-T4 and T5-P3-Pz-P4-T6 electrodes. The light area surrounding each trace represents the SEM. All traces were latency-normalized according to the N2 peak. Amplitude of the N2–P2 response did not differ between Spindle and No Spindle conditions, whereas the P3 amplitude was significantly enhanced in the Spindle condition ($P < 0.0001$). ***C***, 3-D difference topographic maps between the two conditions at the latencies of N2, P2 and P3 components.

Table 1. Latencies and amplitudes of frontal (F), central (C) and parietal (P) responses to nociceptive stimuli in the surface experiment according to the stimulus condition

	Spindle			No spindle		
	F	C	P	F	C	P
Latencies (ms)						
N2	216 ± 10	219 ± 9	221 ± 9	217 ± 13	217 ± 12	218 ± 11
P2	279 ± 15	277 ± 15	280 ± 15	289 ± 16	288 ± 15	285 ± 16
P3	572 ± 24	574 ± 25	576 ± 24	560 ± 20	560 ± 20	562 ± 20
Amplitudes (μV)						
N2–P2	12.3 ± 2.6	16.5 ± 3.5	17.6 ± 3.4	9.9 ± 2.6	13.4 ± 3.1	12.4 ± 3.5
P3	11.6 ± 3.6	20.9 ± 3.3	26.7 ± 4.0	9.6 ± 2.4	12.3 ± 2.6	12.8 ± 2.4

Data are the mean ± SEM.

cortical arousals and awakenings were similar regardless of whether nociceptive stimuli were delivered during spindling activity or apart from it. Unexpectedly, the effect of spindles on arousals induced by sensory stimuli has not been assessed previously in humans. This might be explained by the fact that sensory input in previous sleep studies was mainly auditory (Yamadori, 1971; Elton *et al.* 1997; Cote *et al.* 2000; Schabus *et al.* 2012), a modality that barely interrupts sleep (Bastuji *et al.* 1995; Lavigne *et al.* 2004), in contrast to somatic stimuli at nociceptive threshold, which induce arousals in ∼30% of trials (Lavigne *et al.* 2004; Bastuji *et al.* 2008; Mazza *et al.* 2012). As a result of the lack of genuine arousals, most previous studies used K-complex induction as a surrogate marker of sleep disruption. Considering K-complex as an indicator of arousal remains a matter of debate (Amzica & Steriade, 2002; Halász *et al.* 2004; Colrain, 2005) and reports on their behaviour to external stimuli remain controversial. Although Yamadori (1971) reported 'suppression' of K-complexes when auditory stimuli occurred during spindles, in contrast, Church *et al.* (1978) found an increase in K-complexes with spindles, and Crowley *et al.* (2004) did not describe any consistent effect of spindle on K-complex generation.

Cardiac activation follows any intruding sensory stimulation during sleep, especially when the stimulus is nociceptive (Halász *et al.* 2004). The sympathetic-dependent cardiac reactivity to nociceptive stimulation persists at all sleep stages (Lavigne *et al.* 2001; Chouchou *et al.* 2011) and is modulated by cortical activation (Chouchou *et al.* 2011). In the present study, sleep spindling did not reduce stimulus-driven cardiac activation. This is in accordance with the seminal results reported by Church *et al.* (1978) showing a similar heart

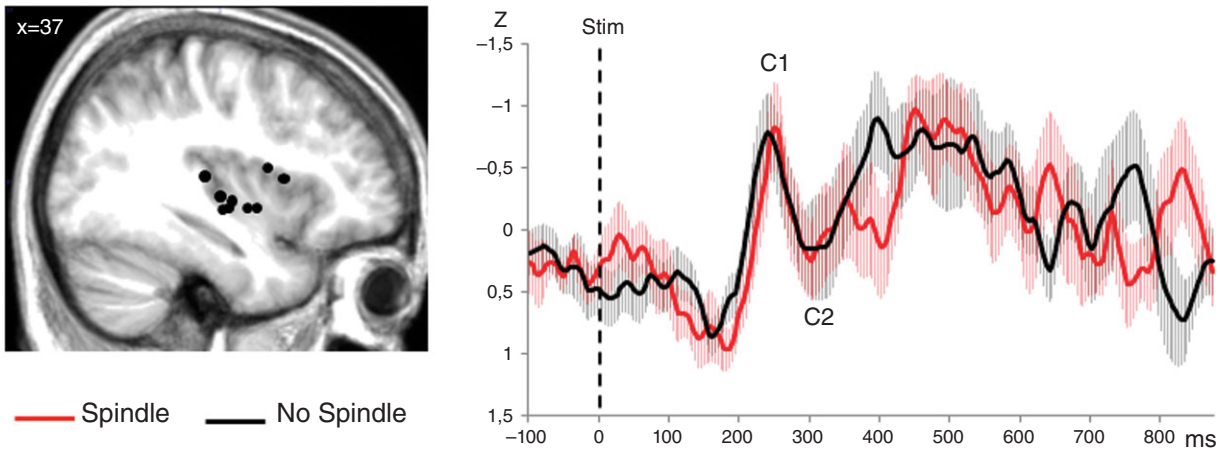

Figure 5. Grand-averages of LEPs (n = 9 patients) recorded within the insular cortex (referential mode) according to stimulus condition
Left: anatomical sites of contacts in the insula (black dots) on a sagittal view of the mean MNI normalized MRI of the nine patients (MNI co-ordinate x = 37). Right: LEPs recorded from the insular cortex. The light area surrounding each trace represents the SEM. All the traces have been latency-normalized according to the C1 peak and amplitude-normalized using the standard score unit (Z-score). The amplitude of the C1–C2 response did not differ between the Spindle and No Spindle conditions.

Table 2. Latencies and amplitudes (before standardization) of the insular response to nociceptive stimuli according to the stimulus condition

	Spindle	No spindle
Latencies (ms)		
C1	239 ± 15	231 ± 10
C2	288 ± 16	275 ± 11
Amplitudes (μV)		
C1–C2	31.6 ± 5.7	23.2 ± 4.4

Data are the mean ± SEM.

rate increase to auditory stimuli during or apart from sleep spindles. In sum, our results strongly suggest that the neuronal mechanisms sustaining spindling activity do not influence those involved in behavioural or autonomic reactivity to intruding nociceptive stimuli during sleep stage N2.

The absence of inhibitory effect of spindling on nociceptive processing was also reflected on electrophysiological grounds, which demonstrated that the earliest steps of cortical processing remained unchanged regardless of whether or not laser stimuli were concomitant to spindles. This remained true if the spindle was present within the thalamus or in the cortex when the nociceptive input occurred. The posterior insular cortex, known to receive ∼40% of spinothalamic input in primates (Dum *et al.* 2009), is one cortical area responding systematically to nociceptive phasic stimuli, both during waking and sleep (Garcia-Larrea & Peyron, 2013). The fact that spindle activity failed to modify either the insular nociceptive response, recorded intracortically, or the ensuing associative components recorded from the surface, indicates that nociceptive inputs reached the cortex without specific attenuation, even when a spindle was present within the thalamus. Again, our results differ from those reported in the context of auditory stimulation, which have often suggested some inhibitory effect of cortically detected spindles on electrophysiological (Elton *et al.* 1997; Cote *et al.* 2000; Schabus *et al.* 2012) or metabolic responses (Schabus *et al.* 2012). The difference in stimulus presentation between the present study and that of previous reports may account for part of this inconsistency because the interstimulus interval was much slower in the present study than in most of previous reports using auditory ones (i.e. >10 s *vs.* ≤3 s). In our case, this longer interstimulus interval allowed an untying the effect of spindle from that of habituation related to the repetition of the stimuli. Also, suprathreshold nociceptive stimuli at rates faster than 0.2 Hz tend to create wind-up phenomena, already arising at spinal level, which would have complicated the interpretation of results. Such a discrepancy between auditory studies and the results of the present study may also relate to the unique homeostatic relevance of nociception, where alerting capacities are essential for survival. Differences in sensory systems carrying noxious and non-noxious information are particularly apparent in their differing GABAergic circuitry within the thalamus. The synaptic relationships of non-nociceptive thalamic terminals take the form of 'triads', whereby the ascending axon simultaneously activates thalamocortical relay neurons and the dendritic appendages of inhibitory GABA interneurons (Ralston & Ralston, 1994). However, this arrangement, considered to mediate feed forward inhibition of thalamocortical cells (Ohara & Lieberman, 1993), is absent in more than 85% of spinothalamic afferents, which form simple axodendritic synapses with relay cells, and do not contact inhibitory GABA interneurons (Ralston & Ralston, 1994). Such a simple circuitry suggests that the transmission of noxious information is much less subject to GABAergic interneuronal modulation than non-noxious information carried by the lemniscal afferents (Ralston & Ralston, 1994; Ralston, 2005). In anaesthetized rats, nociceptive (but not tactile) input was able to inhibit a significant portion of GABAergic reticular units (Yen & Shaw, 2003) suggesting that the somatosensory reticular thalamus may serve as 'modality gate' by inhibiting tactile inputs at the same time as letting noxious information pass. Thus, lack of inhibitory GABAergic modulation of spinothalamic input by thalamic interneurons and reticular cells might hypothetically explain why the gating role of sleep spindles on synaptic transmission is not effective for nociceptive information.

The enhancement of a late component recorded on the surface at 500–700 ms during spindles was unexpected because such long-latency responses reflect the activation of high-order processing networks linked to the detection of behaviourally relevant input, in both humans (Polich, 2007) and non-human primates (Ueno *et al.* 2010). Such late 'P3' component has been described following nociceptive stimulation in waking subjects, and was considered as an equivalent of the cognitive 'P300', or 'P3b' wave (Lorenz & Garcia-Larrea, 2003), associated with cognitive closure, memory encoding and stimulus access to consciousness (Polich, 2007). The main contributors to P3 generation are multimodal associative cortices, including the temporo-parieto-occipital junction, as well as the anterior and posterior cingulate and prefrontal areas (Halgren *et al.* 1998; Brázdil *et al.* 2005), and this may explain why it was easily detected on the scalp but not in intra-insular recordings, which may not participate in these high-order networks. P3-like activity has been shown to persist during sleep in response to behaviourally significant stimuli, even if subjects do not remember the stimulus on awakening (Perrin *et al.* 1999; Bastuji *et al.* 2003), and its presence was associated with the occurrence of arousals after nociceptive stimuli (Bastuji

et al. 2008). Thus, an analysis of the relationship between P3 modulation, arousal reactions and spindle should be appealing, although this would have required more stimuli in each condition.

In our subjects, P3 enhancement to noxious stimuli delivered during spindling suggests that spindles not only failed to prevent the activation of sensory and associative processing of noxious input, but also enhanced such processing compared to non-spindling sleep periods. Although this view challenges existing ideas on spindle functionality, a possible role of spindling in promoting, rather than depressing, some cortical functions has also been supported by the association between enhanced sleep spindling and improvement of explicit and procedural memory consolidation (Diekelmann & Born, 2010; Fogel & Smith, 2011; Rasch & Born, 2013). These results, together with our own, also concur with data suggesting that sleep spindles may participate in cortical-generated gamma activity (Puig *et al.* 2008), as well as with experiments in cats showing increased synaptic plasticity during spindles (Timofeev *et al.* 2002).

Sleep spindles are known to be associated with sleep slow oscillations in a dynamic interaction between the thalamus and the cortex (Crunelli & Hughes, 2010) and appear to be preferentially synchronized to the depolarizing slow oscillation phase commonly labelled 'up-state' (Mölle *et al.* 2011). Failure to disentangle the relationship between spindling and up- or down-states in slow oscillations is clearly a limitation of the present study because up-states are associated with depolarization and vigorous firing, whereas, in down-states, the membrane potential is hyperpolarized and neuronal firing fades. Unfortunately, the sufficient number of stimuli delivered per subject, and especially during N3, needed to investigate the effect of the interaction between spindle and such ultra-slow sleep oscillation on nociceptive responses is lacking in the present data. Two studies, one in humans (Massimini *et al.* 2003) the other in cats (Rosanova & Timofeev, 2005), showed an influence of slow oscillations on non-nociceptive cortical responses, although the exact role of the combined slow wave/spindle activities on nociceptive input could not be assessed in the present study and remains to be clarified.

Conclusions

Sleep spindles detected in the thalamus or cortex failed to depress arousal reactions, cardiovascular activation or cortical responses to nociceptive stimuli, and could even enhance late associative responses. This may reflect the unique homeostatic relevance of nociception for survival, requiring 'open access' to higher centres even during sleep. It also shows that, under particular circumstances, sleep spindles do not act as sensory suppressors but may respect or even enhance sensory transmission.

References

Amzica F & Steriade M (2002). The functional significance of K-complexes. *Sleep Med Rev* **6**, 139–149.

Astori S, Wimmer RD & Lüthi A (2013). Manipulating sleep spindles – expanding views on sleep, memory, and disease. *Trends Neurosci* **36**, 738–748.

Bastuji H, Frot M, Mazza S, Perchet C, Magnin M & Garcia-Larrea L (2015). Thalamic responses to nociceptive-specific input in humans: functional dichotomies and thalamo-cortical connectivity. *Cereb Cortex* doi: 10.1093/cercor/bhv106.

Bastuji H, García-Larrea L, Franc C & Mauguière F (1995). Brain processing of stimulus deviance during slow-wave and paradoxical sleep: a study of human auditory evoked responses using the oddball paradigm. *J Clin Neurophysiol* **12**, 155–167.

Bastuji H, Mazza S, Perchet C, Frot M, Mauguière F, Magnin M & Garcia-Larrea L (2012). Filtering the reality: functional dissociation of lateral and medial pain systems during sleep in humans. *Hum Brain Mapp* **33**, 2638–2649.

Bastuji H, Perchet C, Legrain V, Montes C & Garcia-Larrea L (2008). Laser evoked responses to painful stimulation persist during sleep and predict subsequent arousals. *Pain* **137**, 589–599.

Bastuji H, Perrin F & Garcia-Larrea L (2003). Event-related potentials during forced awakening: a tool for the study of acute sleep inertia. *J Sleep Res* **12**, 189–206.

Brázdil M, Dobsík M, Mikl M, Hlustík P, Daniel P, Pazourková M, Krupa P & Rektor I (2005). Combined event-related fMRI and intracerebral ERP study of an auditory oddball task. *Neuroimage* **26**, 285–293.

Chouchou F, Pichot V, Perchet C, Legrain V, Garcia-Larrea L, Roche F & Bastuji H (2011). Autonomic pain responses during sleep: a study of heart rate variability. *Eur J Pain* **15**, 554–560.

Church MW, Johnson LC & Seales DM (1978). Evoked K-complexes and cardiovascular responses to spindle-synchronous and spindle-asynchronous stimulus clicks during NREM sleep. *Electroencephalogr Clin Neurophysiol* **45**, 443–453.

Colrain IM (2005). The K-complex: a 7-decade history. *Sleep* **28**, 255–273.

Cote KA, Epps TM & Campbell KB (2000). The role of the spindle in human information processing of high-intensity stimuli during sleep. *J Sleep Res* **9**, 19–26.

Crowley K, Trinder J & Colrain IM (2004). Evoked K-complex generation: the impact of sleep spindles and age. *Clin Neurophysiol* **115**, 471–476.

Cruccu G, Aminoff MJ, Curio G, Guerit JM, Kakigi R, Mauguiere F, Rossini PM, Treede R-D & Garcia-Larrea L (2008). Recommendations for the clinical use of somatosensory-evoked potentials. *Clin Neurophysiol* **119**, 1705–1719.

Crunelli V & Hughes SW (2010). The slow (<1 Hz) rhythm of non-REM sleep: a dialogue between three cardinal oscillators. *Nat Neurosci* **13**, 9–17.

Dang-Vu TT, Bonjean M, Schabus M, Boly M, Darsaud A, Desseilles M, Degueldre C, Balteau E, Phillips C, Luxen A, Sejnowski TJ & Maquet P (2011). Interplay between spontaneous and induced brain activity during human non-rapid eye movement sleep. *Proc Natl Acad Sci USA* **108**, 15438–15443.

Dang-Vu TT, McKinney SM, Buxton OM, Solet JM & Ellenbogen JM (2010). Spontaneous brain rhythms predict sleep stability in the face of noise. *Curr Biol* **20**, R626–R627.

Diekelmann S & Born J (2010). The memory function of sleep. *Nat Rev Neurosci* **11**, 114–126.

Dum RP, Levinthal DJ & Strick PL (2009). The spinothalamic system targets motor and sensory areas in the cerebral cortex of monkeys. *J Neurosci* **29**, 14223–14235.

Elton M, Winter O, Heslenfeld D, Loewy D, Campbell K & Kok A (1997). Event-related potentials to tones in the absence and presence of sleep spindles. *J Sleep Res* **6**, 78–83.

Fogel SM & Smith CT (2011). The function of the sleep spindle: a physiological index of intelligence and a mechanism for sleep-dependent memory consolidation. *Neurosci Biobehav Rev* **35**, 1154–1165.

Frot M, Faillenot I & Mauguière F (2014). Processing of nociceptive input from posterior to anterior insula in humans. *Hum Brain Mapp* **35**, 5486–5499.

Garcia-Larrea L & Peyron R (2013). Pain matrices and neuropathic pain matrices: a review. *Pain* **154**(Suppl 1), S29–S43.

De Gennaro L & Ferrara M (2003). Sleep spindles: an overview. *Sleep Med Rev* **7**, 423–440.

Goodin D, Desmedt J, Maurer K & Nuwer MR (1994). IFCN recommended standards for long-latency auditory event-related potentials. Report of an IFCN committee. International Federation of Clinical Neurophysiology. *Electroencephalogr Clin Neurophysiol* **91**, 18–20.

Guenot M, Isnard J, Ryvlin P, Fischer C, Ostrowsky K, Mauguiere F & Sindou M (2001). Neurophysiological monitoring for epilepsy surgery: the Talairach SEEG method. StereoElectroEncephaloGraphy. Indications, results, complications and therapeutic applications in a series of 100 consecutive cases. *Stereotact Funct Neurosurg* **77**, 29–32.

Halász P, Terzano M, Parrino L & Bódizs R (2004). The nature of arousal in sleep. *J Sleep Res* **13**, 1–23.

Halgren E, Marinkovic K & Chauvel P (1998). Generators of the late cognitive potentials in auditory and visual oddball tasks. *Electroencephalogr Clin Neurophysiol* **106**, 156–164.

Iber C, Ancoli-Israel S, Chesson A & Quan SF for the american academy of sleep medicine (2007). *The AASM manual for the scoring of sleep and associated events: rules, terminology and technical specifications*, 1st edn. Westchester, IL: American Academy of Sleep Medicine.

Lavigne G, Brousseau M, Kato T, Mayer P, Manzini C, Guitard F & Monplaisir J (2004). Experimental pain perception remains equally active over all sleep stages. *Pain* **110**, 646–655.

Lavigne GJ, Zucconi M, Castronovo V, Manzini C, Veglia F, Smirne S & Ferini-Strambi L (2001). Heart rate changes during sleep in response to experimental thermal (nociceptive) stimulations in healthy subjects. *Clin Neurophysiol* **112**, 532–535.

Leandri M, Saturno M, Spadavecchia L, Iannetti GD, Cruccu G & Truini A (2006). Measurement of skin temperature after infrared laser stimulation. *Neurophysiol Clin* **36**, 207–218.

Loomis AL, Harvey EN & Hobart G (1935). Potential rhythms of the cerebral cortex during sleep. *Science* **81**, 597–598.

Lorenz J & Garcia-Larrea L (2003). Contribution of attentional and cognitive factors to laser evoked brain potentials. *Neurophysiol Clin* **33**, 293–301.

Magnin M, Bastuji H, Garcia-Larrea L & Mauguière F (2004). Human thalamic medial pulvinar nucleus is not activated during paradoxical sleep. *Cereb Cortex* **14**, 858–862.

Massimini M, Rosanova M & Mariotti M (2003). EEG slow (approximately 1 Hz) waves are associated with nonstationarity of thalamo-cortical sensory processing in the sleeping human. *J Neurophysiol* **89**, 1205–1213.

Mazza S, Magnin M & Bastuji H (2012). Pain and sleep: from reaction to action. *Neurophysiol Clin* **42**, 337–344.

Mölle M, Bergmann TO, Marshall L & Born J (2011). Fast and slow spindles during the sleep slow oscillation: disparate coalescence and engagement in memory processing. *Sleep* **34**, 1411–1421.

Morel A, Magnin M & Jeanmonod D (1997). Multiarchitectonic and stereotactic atlas of the human thalamus. *J Comp Neurol* **387**, 588–630.

Moruzzi G, Brookhart JM, Niemer WT & Magoun HW (1950). Augmentation of evoked electro-cortical activity during spindle bursts. *Electroencephalogr Clin Neurophysiol* **2**, 29–31.

Ohara PT & Lieberman AR (1993). Some aspects of the synaptic circuitry underlying inhibition in the ventrobasal thalamus. *J Neurocytol* **22**, 815–825.

Ostrowsky K, Magnin M, Ryvlin P, Isnard J, Guenot M & Mauguière F (2002). Representation of pain and somatic sensation in the human insula: a study of responses to direct electrical cortical stimulation. *Cereb Cortex* **12**, 376–385.

Perchet C, Godinho F, Mazza S, Frot M, Legrain V, Magnin M & Garcia-Larrea L (2008). Evoked potentials to nociceptive stimuli delivered by CO_2 or Nd:YAP lasers. *Clin Neurophysiol* **119**, 2615–2622.

Perrin F, García-Larrea L, Mauguière F & Bastuji H (1999). A differential brain response to the subject's own name persists during sleep. *Clin Neurophysiol* **110**, 2153–2164.

Polich J (2007). Updating P300: an integrative theory of P3a and P3b. *Clin Neurophysiol* **118**, 2128–2148.

Puig MV, Ushimaru M & Kawaguchi Y (2008). Two distinct activity patterns of fast-spiking interneurons during neocortical UP states. *Proc Natl Acad Sci USA* **105**, 8428–8433.

Ralston HJ (2005). Pain and the primate thalamus. *Prog Brain Res* **149**, 1–10.

Ralston HJ & Ralston DD (1994). Medial lemniscal and spinal projections to the macaque thalamus: an electron microscopic study of differing GABAergic circuitry serving thalamic somatosensory mechanisms. *J Neurosci* **14**, 2485–2502.

Rasch B & Born J (2013). About sleep's role in memory. *Physiol Rev* **93**, 681–766.

Rorden C & Brett M (2000). Stereotaxic display of brain lesions. *Behav Neurol* **12**, 191–200.

Rosanova M & Timofeev I (2005). Neuronal mechanisms mediating the variability of somatosensory evoked potentials during sleep oscillations in cats. *J Physiol* **562**, 569–582.

Rosenberg DS, Mauguière F, Catenoix H, Faillenot I & Magnin M (2009). Reciprocal thalamocortical connectivity of the medial pulvinar: a depth stimulation and evoked potential study in human brain. *Cereb Cortex* **19**, 1462–1473.

Schabus M, Dang-Vu TT, Heib DPJ, Boly M, Desseilles M, Vandewalle G, Schmidt C, Albouy G, Darsaud A, Gais S, Degueldre C, Balteau E, Phillips C, Luxen A & Maquet P (2012). The fate of incoming stimuli during NREM sleep is determined by spindles and the phase of the slow oscillation. *Front Neurol* **3**, 40.

Schwarz S, Greffrath W, Büsselberg D & Treede RD (2000). Inactivation and tachyphylaxis of heat-evoked inward currents in nociceptive primary sensory neurones of rats. *J Physiol (Lond)* **528**, 539–549.

Steriade M (2006). Grouping of brain rhythms in corticothalamic systems. *Neuroscience* **137**, 1087–1106.

Talairach J & Bancaud J (1973). Stereotactic approach to epilepsy: methodology of anatomo-functional stereotaxic investigations. *Prog Neurol Surg* **5**, 297–354.

Timofeev I, Grenier F, Bazhenov M, Houweling AR, Sejnowski TJ & Steriade M (2002). Short- and medium-term plasticity associated with augmenting responses in cortical slabs and spindles in intact cortex of cats in vivo. *J Physiol (Lond)* **542**, 583–598.

Ueno A, Hirata S, Fuwa K, Sugama K, Kusunoki K, Matsuda G, Fukushima H, Hiraki K, Tomonaga M & Hasegawa T (2010). Brain activity in an awake chimpanzee in response to the sound of her own name. *Biol Lett* **6**, 311–313.

Warby SC, Wendt SL, Welinder P, Munk EGS, Carrillo O, Sorensen HBD, Jennum P, Peppard PE, Perona P & Mignot E (2014). Sleep-spindle detection: crowdsourcing and evaluating performance of experts, non-experts and automated methods. *Nat Methods* **11**, 385–392.

Yamadori A (1971). Role of the spindles in the onset of sleep. *Kobe J Med Sci* **17**, 97–111.

Yen C-T & Shaw F-Z (2003). Reticular thalamic responses to nociceptive inputs in anesthetized rats. *Brain Res* **968**, 179–191.

Additional information

Competing interests

The authors declare that they have no competing interests.

Author contributions

LG-L, SM and HB conceived and designed the experiments. LC, MC, CP, SM and HB performed the experiments. LC, FC, GP, MC, BDB, SM and HB analysed the data. LC, FC, CP, LG-L, SM and HB wrote the paper. All authors have approved the final version of the manuscript and agree to be accountable for all aspects of the work. All persons designated as authors qualify for authorship, and all those who qualify for authorship are listed.

Funding

The study was supported by a Region Rhone-Alpes/France ARC2 2012–2015 scholarship (LC), an INSERM interface contract Grant (HB) and by grants from the French Society for Pain Evaluation and Therapy (Translational Research Grant 2012–14) and the Laboratory of Excellence (LABEX) CORTEX (ANR-11-LABX-0042; ANR-11-IDEX-0007).

Acknowledgements

We thank M. Magnin for his valuable advice. We are indebted to Drs J. Isnard and P. Ryvlin for the opportunity to study their patients, as well as to Dr M. Guenot for stereotactic electrode implantations.